Cold Atomic Collisions: Coherent Control of Penning and Associative Ionization

Carlos A. Arango,[1] Moshe Shapiro,[2,3] and Paul Brumer[1]

[1]*Chemical Physics Theory Group, Department of Chemistry, and Center for Quantum Information and Quantum Control, University of Toronto, Toronto M5S3H6, Canada*
[2]*Department of Chemical Physics, The Weizmann Institute, Rehovot 76100, Israel*
[3]*Department of Chemistry, The University of British Columbia, Vancouver V6T1Z1, Canada*

Coherent control techniques are computationally applied to cold (1 mK $< T <$ 1 K) and ultracold ($T <$ 1 μK) Ne*$(3s, {}^3P_2)$ + Ar$({}^1S_0)$ collisions. We show that by using various initial superpositions of the Ne*$(3s, {}^3P_2)$ $M = \{-2, -1, 0, 1, 2\}$ Zeeman sublevels it is possible to reduce the Penning ionization and associative ionization cross sections by as much as 4 orders of magnitude. It is also possible to drastically change the ratio of these two processes. The results are based on combining, within the "rotating atom approximation", empirical and *ab initio* ionization widths.

Cold and ultracold atomic processes present a new laboratory environment in which to explore and utilize the quantum nature of matter. In this Letter we show that the significance of quantum effects in such systems permit unprecedented control over collisional processes. In particular, we consider the theory and computational implementation of the coherent control [1–4] of absolute and relative cross sections in the collision of metastable atoms A^* and ground state target atoms B. Such collisions can result in two main channels: (1) the ionization of the target atom and the deexcitation of the metastable species, i.e., Penning ionization (PI) [5], or (2) associative ionization (AI), wherein the colliding partners form an ionic dimer while emitting an energetic electron. Schematically,

$$\text{(AI)}\, AB^+ + e^- \leftarrow A^* + B \rightarrow A + B^+ + e^-, \text{(PI)}. \quad (1)$$
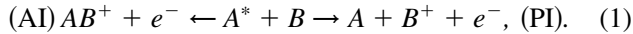
As an example, we consider the coherent control of PI and AI resulting from collisions between Ne*$(3s, {}^3P_2)$ and Ar$({}^1S_0)$ in the cold and ultracold regimes. Amongst other observations, the suppression of these processes in favor of elastic scattering may well prove useful for the production of Bose-Einstein condensates of excited states atoms.

A wealth of experimental information and theoretical calculations on the uncontrolled Ne* + Ar collisions is available and the possibility of control of this system at thermal energies [6] now exists. As we report below, the control achievable in the sub mK regime is far more impressive.

The initial superposition state.—Coherent control is achieved by preparing the colliding pair in an initial superposition of internal states, such as,

$$|\psi\rangle = e^{i\mathbf{K}\cdot\mathbf{R}_{\text{c.m.}} + i\mathbf{k}\cdot\mathbf{r}}|\phi_{\text{Ar}}\rangle \sum_M a_M |\phi_{\text{Ne}^*}^M\rangle, \quad (2)$$

where $|\psi_{\text{Ar}}\rangle$ is the initial state of the Ar atom and $|\phi_{\text{Ne}^*}^M\rangle$, are Ne* Zeeman sublevels, with $M = \{-2, -1, 0, 1, 2\}$ being the projection of the Ne* electronic angular momentum on the space-fixed quantization axis. a_M are prepara-

tion coefficients, to be optimized to yield a desired objective, $\mathbf{R}_{\text{c.m.}}$ is the c.m. coordinate, $\mathbf{R}_{\text{c.m.}} \equiv (m_{\text{Ne}}\mathbf{r}^{\text{Ne}} + m_{\text{Ar}}\mathbf{r}^{\text{Ar}})/(m_{\text{Ne}} + m_{\text{Ar}})$, and $\mathbf{r}$ is the internuclear separation vector, $\mathbf{r} \equiv \mathbf{r}^{\text{Ne}} - \mathbf{r}^{\text{Ar}}$. The (body-fixed) momenta are given as, $\mathbf{K} \equiv \mathbf{k}^{\text{Ne}} + \mathbf{k}^{\text{Ar}}$, $\mathbf{k} \equiv (m_{\text{Ar}}\mathbf{k}^{\text{Ne}} - m_{\text{Ne}}\mathbf{k}^{\text{Ar}})/(m_{\text{Ne}} + m_{\text{Ar}})$. Here $\mathbf{r}^{\text{Ar}}$ and $\mathbf{k}^{\text{Ar}}$ ($\mathbf{r}^{\text{Ne}}$ and $\mathbf{k}^{\text{Ne}}$) denote the position and momentum of the Ar (Ne*) atom in the laboratory frame. Note that the fact that the initial superposition state is comprised of degenerate M states, and that the collision partners are atoms, ensures that the conditions for coherent control [3] are satisfied.

The rates of the PI and AI processes mainly depend on λ, the body-fixed (BF) projection of the electronic angular momentum on $\mathbf{r}$, the interatomic axis. It is therefore necessary to express the $|\phi_{\text{Ne}^*}^M\rangle$ states in terms of the $|\phi_{\text{Ne}^*}^\lambda\rangle$ BF states. We adopt the rotating atom approximation [7] according to which the axis of quantization of the electrons faithfully follows the internuclear separation vector. This establishes a 1:1 correspondence between the M values and the λ values as the atoms approach one another. Hence, the (even parity) linear combination in the BF frame is written as,

$$|\psi\rangle = |\phi_{\text{Ar}}\rangle e^{i\mathbf{K}\cdot\mathbf{R}_{\text{c.m.}} + i\mathbf{k}\cdot\mathbf{r}} \sum_{\Omega=0}^{2} |\phi_{\text{Ne}^*}^\Omega\rangle a_\Omega, \quad (3)$$

where $\Omega \equiv |\lambda|$, and (due to the assumed even parity) $a_\Omega \equiv (a_M + a_{-M})$.

Scattering theory.—The basic formulae for our purposes are found in Refs. [8–10] giving the scattering amplitudes for PI and AI based on O'Malley's theory of dissociative attachment [11,12]. Prior to the collision, the internuclear momentum vector $\mathbf{k}$ has magnitude k and direction $\hat{\mathbf{k}}$. Here k is given in units of temperature. After the collision, its magnitude is k_f and its direction is $\hat{\mathbf{k}}_f$. Asymptotically, the Penning electron departs along the $\hat{\mathbf{k}}_\varepsilon$ direction with energy ε. The energy of the emitted electron is related to the collisional energy E and the energy of the nuclei after the

collision E' by the conservation of energy $E + \varepsilon_0 = \varepsilon + E'$, with $\varepsilon_0 = E_* - IE$ being the difference between the excitation energy of the metastable Ne* atom and the ionization energy of the target Ar atom.

The scattering amplitude, which is exact within the Born-Oppenheimer approximation, is given by [8,9,13]

$$f(\hat{\mathbf{k}}_f, \varepsilon, \hat{\mathbf{k}}_\varepsilon; \mathbf{k}) = -\frac{2M_r \rho_\varepsilon^{1/2}}{(4\pi\hbar)^2}\left(\frac{k_f}{k}\right)^{1/2}\langle\psi_\varepsilon|V_{\varepsilon,\hat{\mathbf{k}}_\varepsilon}|\psi_d\rangle, \quad (4)$$

where M_r is the reduced mass of the nuclei and ρ_ε is the density of electronic continuous states. $\psi_d(\mathbf{r})$ is the incoming wave function calculated on the optical potential $V_*(r) - \frac{i}{2}\Gamma(r)$ and $\psi_\varepsilon(\mathbf{r})$ describes the system on the exit channel $V_+(r)$. The electronic part is completely included in $V_{\varepsilon,\hat{\mathbf{k}}_\varepsilon}(\mathbf{r})$, which is the probability amplitude for the emission of an electron with ε, and $\hat{\mathbf{k}}_\varepsilon$.

Partial-wave expansions of $\psi_\varepsilon(\mathbf{r})$, $V_{\varepsilon,\hat{\varepsilon}}(\mathbf{r})$, and $\psi_d(\mathbf{r})$, and the evaluation of the integral over $\mathbf{r}$ will give, for the special case when the space-fixed z axis is along $\mathbf{k}$,

$$f = \frac{\pi^{1/2}}{ik}\sum_{\ell,\mu,l,l'} i^{l-l'}(2l+1)(2l'+1)^{1/2}\begin{pmatrix} l' & \ell & l \\ 0 & 0 & 0 \end{pmatrix}$$

$$\times \begin{pmatrix} l' & \ell & l \\ -\mu & \mu & 0 \end{pmatrix}S_{l'\ell}^l(\varepsilon)Y_{l'-\mu}(\hat{\mathbf{k}}_f)Y_{\ell\mu}(\hat{\mathbf{k}}_\varepsilon), \quad (5)$$

with the partial-wave S matrix in terms of the phase shifts δ^l and $\delta_f^{l'}$ of the radial partial-wave components ψ_d^l and $\psi^{l'}$

$$S_{l'\ell}^l(\varepsilon) = -i\frac{4M_r\rho_\varepsilon^{1/2}}{\hbar^2}e^{i(\delta^l+\delta_f^{l'})}\langle\psi_\varepsilon^{l'}|V_{\varepsilon\ell}|\psi_d^l\rangle, \quad (6)$$

where $V_{\varepsilon\ell}(r) \approx \alpha_\ell[\Gamma(r)/2\pi]^{1/2}$.

For crossed beams, in the rotating atom approximation, we find that the scattering amplitude for a linear superposition $\mathbf{a}_\Omega$ can be written as

$$f_a(\hat{k}_f, \varepsilon, \hat{\mathbf{k}}_\varepsilon, k) = \sum_\Omega a_\Omega f_\Omega(\hat{k}_f, \varepsilon, \hat{\mathbf{k}}_\varepsilon, k), \quad (7)$$

with $f_\Omega(\hat{k}_f, \varepsilon, \hat{\varepsilon}; k, \Omega)$ given by Eq. (5) and $S_{l'\ell}^l(\varepsilon)$ replaced by

$$S_{l'\ell}^{l,\Omega}(\varepsilon) = -2i\frac{2M_r\rho_\varepsilon^{1/2}}{\hbar^2}e^{i(\delta^l+\delta_f^{l'})}\langle\psi_\varepsilon^{l'}|V_{\varepsilon\ell}^\Omega|\psi_d^l\rangle, \quad (8)$$

for PI, and

$$S_{l'\ell}^{l,\Omega}(\varepsilon) = -2i\left(\frac{2M_r\pi\rho_\varepsilon}{\hbar^2}\right)^{1/2}e^{i\delta^l}\langle\psi_{v'l'}|V_{\varepsilon\ell}^\Omega|\psi_d^l\rangle, \quad (9)$$

for AI [14]. The $V_{\varepsilon\ell}^\Omega(r)$ matrix elements are related to the ionization widths, $\Gamma_\Omega(r)$ as [5,8,9], $V_{\varepsilon\ell}^\Omega(r) \approx \alpha_\ell[\Gamma_\Omega(r)/2\pi]^{1/2}$. The Γ_Ω are obtained as in Ref. [6], using methods in [14–17].

The differential cross section for PI is obtained by squaring the scattering amplitude Eq. (5). In the rotating atom approximation we obtain

$$\sigma_q(\hat{\mathbf{k}}_f, \varepsilon, \hat{\mathbf{k}}_\varepsilon; k, \mathbf{a}_\Omega) = \left|\sum_\Omega a_\Omega f_{q\Omega}(\hat{\mathbf{k}}_f, \varepsilon, \hat{\mathbf{k}}_\varepsilon; k)\right|^2, \quad (10)$$

where q indicates the exit channel. There are three possible exit channels characterized by the electronic state of the products: $X^2\Sigma_{1/2}^+$, $A_1{}^2\Pi_{3/2}$, and $A_2{}^2\Sigma_{1/2}$. The entrance channel optical potential is connected with each of the exit channels using Morgner's Γ splitting [18,19]. We use optical potentials for the entrance channel derived directly from experiment [14,15]. Since data is available only for scattering experiments at thermal energies (above 1 K), the optical potentials do not include effects associated with very slowly moving atoms (e.g., hyperfine interactions).

The sum Eq. (10) can be expanded to give

$$\sigma_q(\hat{\mathbf{k}}_f, \varepsilon, \hat{\mathbf{k}}_\varepsilon; k, \mathbf{a}_\Omega) = \sum_{\Omega\Omega'} a_{\Omega'}^* a_\Omega \sigma_{q\Omega'\Omega} \quad (11)$$

with $\sigma_{q\Omega'\Omega} = f_{q\Omega'}^* f_{q\Omega}$. Since we are interested in the total ionization cross section, we sum over all the exit channels, and integrate over the solid angles $\hat{\mathbf{k}}_\varepsilon$ and $\hat{\mathbf{k}}_f$, and over the emitted electron energy ε. It is easy to see from the form of the scattering amplitude that the integration over the solid angles yields a Kronecker delta function, thus simplifying the expressions for the $f_{q\Omega'}^* f_{q\Omega}$ products to

$$f_{q\Omega'}^* f_{q\Omega} = \frac{\pi}{k^2}\sum_{\ell ll'}(2l+1)(2l'$$

$$+1)\begin{pmatrix} l' & \ell & l \\ 0 & 0 & 0 \end{pmatrix}^2 S_{l'\ell}^{l\Omega'*}(q,\varepsilon)S_{l'\ell}^{l\Omega}(q,\varepsilon). \quad (12)$$

The PI cross section, $\sigma^{\text{PI}}(\mathbf{a}_\Omega)$, obtained after integrating over the energy of the emitted electron and summing over all exit channels, is,

$$\sigma^{\text{PI}}(\mathbf{a}_\Omega) = \sum_{\Omega'\Omega}\mathbf{a}_{\Omega'}^*\mathbf{a}_\Omega\sigma_{\Omega'\Omega}^{\text{PI}}. \quad (13)$$

As a first example, we examine coherent control obtained using only two $\Omega(= 0, 1)$ states [similar results were obtained for the $\Omega(= 0, 2)$ pair, as shown in the tables below], for which

$$\sigma^{\text{PI}}(\mathbf{a}_\Omega) = |a_0|^2\sigma_0^{\text{PI}} + |a_1|^2\sigma_1^{\text{PI}} + 2\,\text{Re}(a_0^* a_1\sigma_{01}^{\text{PI}}), \quad (14)$$

where $\sigma_\Omega^{\text{PI}} = \sigma_{\Omega\Omega}^{\text{PI}}$.

Similar expressions for AI are obtained by summing over the exit channels and bound states,

$$\sigma^{\text{AI}} = |a_0|^2\sigma_0^{\text{AI}} + |a_1|^2\sigma_1^{\text{AI}} + 2\,\text{Re}(a_0^* a_1\sigma_{01}^{\text{AI}}). \quad (15)$$

Note the crucial interference term, dependent on the magnitude and phase of the a_i, which allows control over the cross sections by varying these coefficients.

Computational results.—Although results are reported for collisions at temperatures up to 1 K, our main focus is on cold collisions at a temperature of 1 mK and on ultracold collisions at 1 μK. At the low temperatures consid-
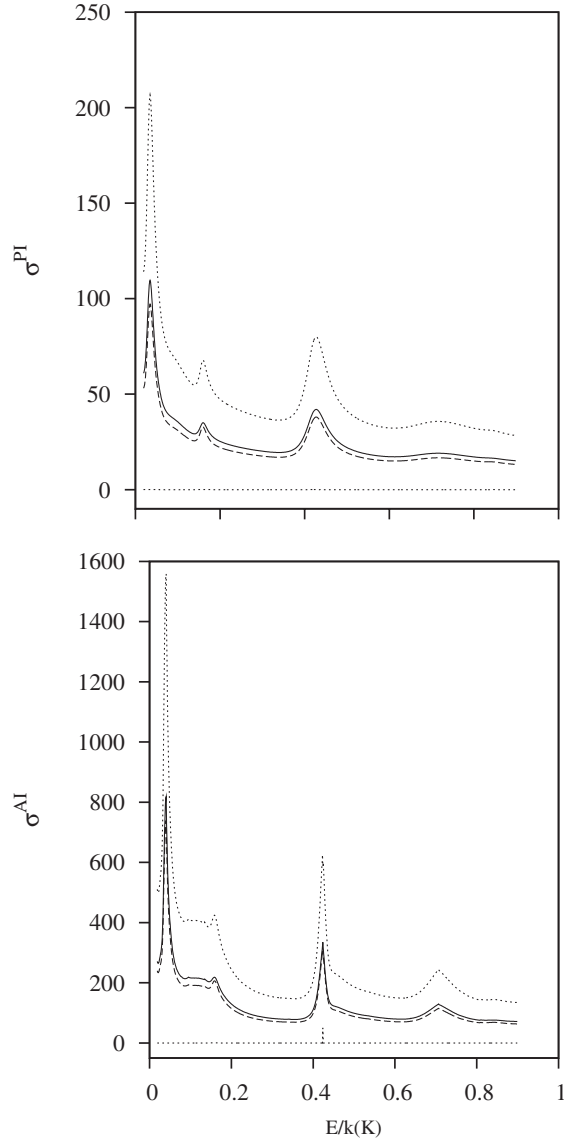
FIG. 1.   PI and AI cross sections for $\Omega = 0, 1$ linear combination. $\Omega = 0$—solid line; $\Omega = 1$ —dashed line; maximum and minimum for the linear combination of $\Omega = 0, 1$—dotted line.

TABLE I.   Cross section for cold collision at $T = 1$ mK. Rows labeled "$\Omega = 0, 1$" and "$\Omega = 0, 2$" show the minimum and maximum of the σ^{PI} and σ^{AI}, obtained by varying the a_i for the indicated superposition.

Ω	σ^{PI} (Å2)	σ^{AI} (Å2)
0	74.68	346.91
1	64.90	306.25
2	13.75	87.01
0,1	1.27×10^{-2}–139.57	3×10^{-2}–653.13
0,2	0.63–87.80	0.60–433.32

in order to control both scattering particles. The internal state superposition can be prepared [21] after cooling while the atoms are trapped in the lattice using, e.g., stimulated Raman adiabatic passage (STIRAP) [22] or coherent population trapping (CPT) [23].

Consider first control results across a broad spectrum of energies up to temperatures of 1 K; Fig. 1 shows the cross sections for $\Omega = 0$ and $\Omega = 1$ scattering as a function of energy. Also shown are the maximum and minimum controlled cross sections (optimized over the a_i coefficients) at each energy for the $\Omega = 0$ plus $\Omega = 1$ linear combination. Several resonances [24] are evident, since the collision

ered, the PI or AI cross sections are very large since the two atoms are in the vicinity of one another for an extended period of time. Further, in the ultracold case only the *s* partial wave contributes, with three angular momentum states contributing in the cold case.

For these energies the relative velocities between the collisional pair are ≈ 1 and ≈ 0.006 m/s, respectively. These relative velocities are experimentally attainable using laser cooling and manipulation techniques. For example, the atoms can be cooled and trapped in a 3D optical lattice, then adiabatically accelerated along a single axis [20]. This setup can reach velocities of up to a few meters per second, and a kinetic energy spread of 150–200 nK around the central beam velocity. The present collisional scenario would require two 3D lattice setups
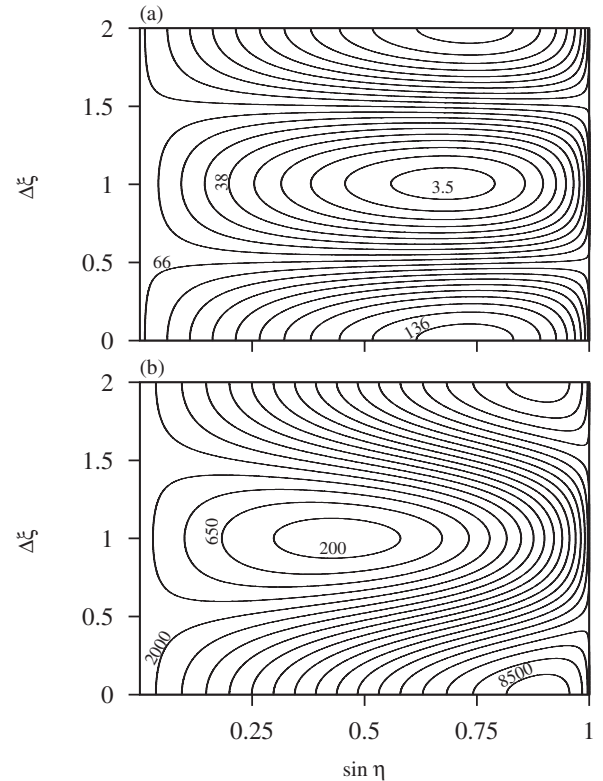

FIG. 2.   Coherent control contours for (a) PI for $\Omega = 0, 1$ in cold collisions at $T = 1$ mK; (b) AI for $\Omega = 0, 2$ in ultracold collisions at $T = 1$ μK. The parameters η and $\Delta\xi$ are defined via: $a_\Omega = \sin\eta e^{i\xi_\Omega}$ and $a_{\Omega'} = \cos\eta e^{i\xi_{\Omega'}}$, with $\Omega, \Omega' = 0, 1, 2$.

TABLE II.   As in Table I, but for ultracold collision at $T = 1 \mu$K.

Ω	σ^{PI} (Å2)	σ^{AI} (Å2)
0	1357.32	7056.92
1	1174.19	6199.40
2	244.27	1728.65
0,1	0.128–2531.38	3.03–13 256.30
0,2	9.88–1591.71	2.28–8783.30

energy is very close to the dissociation threshold for the Ne*-Ar quasimolecule. Noteworthy is that control is extensive, with enhancement and suppression of both cross sections being possible at both resonant and nonresonant energies.

Table I presents numerical results for the cold collision (1 mK) case. We see that it is possible to actively change the AI and PI cross sections by as much as 4 orders of magnitude for the $\Omega = 0, 1$ linear combination and 3 orders of magnitude for the $\Omega = 0, 2$ linear combination. For both linear combinations the position of the minima and maxima for σ^{PI} and σ^{AI} occur at close points in the parameter space (not shown here). A similar observation has been noted at higher temperatures (above 1 K), indicating that both PI and AI cross sections can be controlled simultaneously [6]. Sample results for the control of σ^{PI} as a function of a_i for the cold collision case are shown in Fig. 2(a).

Ultracold collisions, where only s waves contribute to the process, show even more dramatic behavior. As seen in Table II, active changes of up to 4 orders of magnitude, using the $\Omega = 0, 1$ superposition states, and up to 3 orders of magnitude, using the $\Omega = 0, 2$ superposition states, are possible. The AI process can also be almost as well controlled. The resulting σ^{AI} cross sections are shown in Fig. 2(b) for ultracold collisions as function of the a_i. Note that in all cases, the maxima and minima in the control plots (Figs. 1 and 2) are well separated, making the experiment less sensitive to the control parameters.

In summary, we have shown the possibility of a huge range of control of the PI and AI cross sections in Ne* + Ar cold and ultracold collisions. Control is achieved by initiating the collision in a judiciously chosen superposition of Ne* quantum states. Such states can be readily made using new STIRAP techniques [21]. Our results show a wide range of controllability for both PI and AI. For PI the minimum of the cross section is found to be orders of magnitude smaller than the incoherent mixture of $\Omega = 0, 1$ or $\Omega = 0, 2$. In the AI reaction the effects are even more dramatic, showing a minimum 4 orders of magnitude smaller than that of the incoherent mixture $\Omega = 0, 1$ and 3 orders of magnitude smaller than the $\Omega = 0, 2$ mixture.

[1] M. Shapiro and P. Brumer, *Principles of the Quantum Control of Molecular Processes* (John Wiley & Sons, Hoboken, NJ, 2003).
[2] M. Shapiro and P. Brumer, Phys. Rev. Lett. **77**, 2574 (1996).
[3] P. Brumer, A. Abrashkevich, and M. Shapiro, Faraday Discuss. **113**, 291 (1999).
[4] S. Rice and M. Zhao, *Optical Control of Molecular Dynamics* (John Wiley & Sons, Hoboken, NJ, 2000).
[5] P. E. Siska, Rev. Mod. Phys. **65**, 337 (1993).
[6] C. A. Arango, M. Shapiro, and P. Brumer, J. Chem. Phys. (to be published).
[7] M. Mori, T. Watanabe, and K. Katsuura, J. Phys. Soc. Jpn. **19**, 380 (1964).
[8] A. P. Hickman and H. Morgner, J. Phys. B **9**, 1765 (1976).
[9] H. Morgner, J. Phys. B **11**, 269 (1978).
[10] R. J. Bieniek, Phys. Rev. A **18**, 392 (1978).
[11] T. F. O'Malley, Phys. Rev. **150**, 14 (1966).
[12] T. F. O'Malley, Phys. Rev. **156**, 230 (1967).
[13] W. H. Miller, C. A. Slocomb, and H. F. Schaefer III, J. Chem. Phys. **56**, 1347 (1972).
[14] M. J. Verheijen and H. C. W. Beijerinck, Chem. Phys. **102**, 255 (1986).
[15] R. W. Gregor and P. E. Siska, J. Chem. Phys. **74**, 1078 (1981).
[16] E. R. T. Kerstel, M. F. M. Janßens, K. A. H. van Leeuwen, and H. C. W. Beijerinck, Chem. Phys. **119**, 325 (1988).
[17] S. S. O. de Beek, J. P. J. Drießen, S. J. J. M. F. Kokkelmans, W. Boom, H. C. W. Biejerinck, and B. J. Varhaar, Phys. Rev. A **56**, 2792 (1997).
[18] H. Morgner, Comments At. Mol. Phys. **11**, 271 (1982).
[19] H. Morgner, J. Phys. B **18**, 251 (1985).
[20] P. Treutlein, K. Y. Chung, and S. Chu, Phys. Rev. A **63**, 051401 (2001).
[21] M. Heinz, F. Vewinger, U. Schneider, L. Yatsenko, and K. Bergmann, Opt. Commun. **264**, 248 (2006).
[22] K. Bergmann, H. Theuer, and B. W. Shore, Rev. Mod. Phys. **70**, 1003 (1998).
[23] S. Knappe, R. Wynands, J. Kitching, H. G. Robinson, and L. Hollberg, J. Opt. Soc. Am. B **18**, 1545 (2001).
[24] P. Westphal, A. Horn, S. Koch, J. Schmand, and H. J. Andrä, Phys. Rev. A **54**, 4577 (1996).